DFT study adsorption of Hydroxychloroquine for treatment COVID-19 by Al, Si and Si-C doping on carbon nanotube surface: A drug delivery simulation

Zaid H. Al-Sawaff (zaidalsawaff@ntu.edu.iq)
Northern Technical University
Serap Senturk Dalgic
Trakya University
Fatma Kandemirli
Kastamonu University
Majid Monajjemi
Kastamonu University
Fatemeh Mollaamin
Kastamonu University

Research Article

Keywords: COVID-19, Hydroxychloroquine, Drug adsorption, Nanoparticles, Density functional theory, Thermodynamic properties

Posted Date: October 15th, 2021

DOI: https://doi.org/10.21203/rs.3.rs-966611/v1

DFT study adsorption of Hydroxychloroquine for treatment COVID-19 by Al, Si and Si-C doping on carbon nanotube surface: A drug delivery simulation

Zaid H. Al-Sawaff [(1) (2)], Serap Senturk Dalgic[(3)], Fatma Kandemirli[(4)] Majid Monajjemi[(4)], Fatemeh Mollaamin[(4)]

[(1)] Material Science & Engineering Dept., Faculty of Engineering and Architecture, Kastamonu University, Turkey,
[(2)] Medical Instrumentation Technology, Technical Engineering College, Northern Technical University, Mosul, Iraq
[(3)] Department of Physics, Faculty of Science, Trakya University, 22030, Edirne, Turkey
[(4)] Biomedical Engineering Department, Faculty of Engineering & Architecture, Kastamonu University, Kastamonu, Turkey

Corresponding author: Zaid h. Al-Sawaff
E-mail: zaidalsawaff@ntu.edu.iq

Abstract

The aim of this study is to investigate the potential and capability of Al-CNT, Si-CNT, and SiC-NT to detect and adsorb Hydroxychloroquine ($C_{18}H_{26}C_lN_3O$) molecular.
For this purpose, we considered different configurations for adsorbing Hydroxychloroquine drug on the surface of Al-CNT, Si-CNT, and SiC-NT nanocluster.
All considered configurations are optimized using DFT theory at the 6-31G** basis set and M062x level of theory, and then from optimized structures, for each nanoparticle, we selected four stable models for the adsorption of Hydroxychloroquine from (O, N, N, and Cl) sites on the surface the selected nanoparticles.
The calculated results indicate that the distance between nanocluster and drug from N site is lower than from all other locations sites for all investigated nanoparticles, and adsorption of Hydroxychloroquine from N site is more favorable especially for the Al-CNT nanotube.
The adsorption energy, hardness, softness, and fermi energy results reveal that the interaction of Hydroxychloroquine with Al-CNT is stronger than Si-CNT, and SiC-NT.
The results clarify that SiC-NT and Si-CNT are not suitable for Hydroxychloroquine drug adsorption because of the low values of Eads, but Al-CNT is an encouraging adsorbent for this drug as Eads of Hydroxychloroquine/Al-CNT complexes are (-45.07, -15.78, -45.15, -93.53) kcal/mol in the gas phase, and (-43.02, -14.43, -43.86, -88.97) kcal/mol for aqueous solution. The energy gap of the Hydroxychloroquine/Al-CNT system is in the range of 2.32 to 3.84 eV. which is in the range of Al-CNT (2.68).
Besides, the HOMO-LUMO orbitals and electrostatic potential (ESP) plots results show that the maximum positive charge is located around the nanocluster surface and the most negative charge is located around the adsorption position and Hydroxychloroquine drug surface.
As well, the appropriate and spontaneous interaction between Hydroxychloroquine drug and all nanoparticles was confirmed by investigating the quantum chemical molecular descriptors and solvation Gibbs free energies of all atoms.
Al-CNT can be used as an amperometric sensor to detect the Hydroxychloroquine drug molecule. Thus, we propose that the Al-CNT can be a promising candidate as a drug delivery vehicle for Hydroxychloroquine drug molecules.

Keywords: COVID-19; Hydroxychloroquine; Drug adsorption; Nanoparticles; Density functional theory; Thermodynamic properties;

1. Introduction

In 1955 a drug titled Hydroxychloroquine with the chemical formula ($C_{18}H_{26}C_lN_3O$) and the chemical structure (2- [4-[(7-chloroquinolin-4-yl) amino]pentyl-ethylamino] ethanol, was submitted to the World Medicines Committee, and soon this became The drug is preferred due to its excellent safety profile [1], its direct interaction with the DNA of viruses and Plasmodium parasites, and the inhibition of heme polymerization.

These were the main reasons why this drug has been known so quickly [2, 3].

Also, the immunomodulating activity of hydroxychloroquine is associated with a wide series of immune-regulating communities that have been widely discussed in related previous works [4-6].

Many scientific works and research have been carried out to use computational methods to screen molecules to find inhibitors against SARS-CoV-2 main protease [7]. In the same vein, the present work reports the engineering optimization of hydroxychloroquine using the theoretical plane. Then, its interaction and behavior were predicted at the same level of theory using frontier molecular orbitals, as well as the interaction of the drug compound with different groups of nanotubes. This analysis allows us to find the most reactive links against the COVID-19 virus and to find a new compound that matches the required drug delivery speed.

Moreover, the locations of the nucleophilic and electrophilic regions of chloroquine derivatives can be clearly predicted by the different colors detected on the particular molecular electrostatic potential surfaces. All of these calculations can help a lot in the biological part since the use of optimized ligand structures is more accurate in molecular calculations, making the software more reliable to use in structure-based drug design.

With the rapid development of nanoscience, various types of nanostructures such as nanotubes, nanoplates, nanocones, and nanoforms have been greatly investigated as potential candidates in various fields such as drug delivery compounds [8-12], and it has been found that nanotubes and the nanocages are the most Preferred candidates for drug carriers due to their high sensitivity to drug particles, fewer side effects, hydrophobic properties, and unique spherical shape, etc.[13-16].

Lately, the interactions between nanotubes and ligands became an important issue, and they can be used together as drug delivery agents as well as sensors [17-18]. Zigzag type (n,0) nanotubes can be preferred for drug delivery studies because of their unique properties.

The binding energy values of the studied Si and Al bonds suggested that doping of nanotubes enhances the reaction mechanism and modifies the structural, chemical, and electronic properties of the new complexes [19-20]. As during the doping of Al and Si, fullerenes interact with the bonds and the stability of the new complexes will increase, putting the binding energy in the chemiluminescence range [21].

The promising issue for using SiC nanotubes is that they have a high reactivity property than other carbon nanotubes (CNT) that comes because of their high polarity [22, 24]. These individual effects of the SiC nano-tube were the crucial advantages for their applications on the basics of fabrication of chemical adsorbents, and electronic nanodevices [25-26].

Hard and Soft Acids and Bases theory are widely used in chemistry to explain the stability of compounds, reaction mechanisms, and pathways, and the terms hard or soft, and acid or base are used for chemical species where the term hard applies to small, with High charge states, weakly polarizable [27].

This theory is used in contexts where qualitative, rather than quantitative, description helps in understanding the dominant factors that drive chemical properties and reactions, as many experiments have been performed to determine the relative order of transition metal bonds and ions in terms of their hardness and softness [28].

Also, Fermi energy is a concept in quantum mechanics that usually refers to the energy difference between the highest and lowest states of a single particle occupied in a quantum system of un interacted fermions at absolute zero temperature [29].
Models of nanoparticles (CNT) with relatively small sizes compared to the size of the drug compound were used in this study to investigate the possibility of binding more than one nanoparticle to the drug compound at the same time in order to obtain the best-desired results in terms of optimal drug delivery and reducing the toxicity rate to the lowest levels.
The main aim of this study is to investigate the adsorption properties of Hydroxychloroquine drugs on the surface of zigzag (6,0) nanotubes as a test case Al-CNT, Si-CNT, and silicon-carbide nanotube (SiC-NT) to be used as a suitable delivery vehicle for this drug.
In this investigation, the evaluation has been done among many structural and electronic properties before and after the adsorption of Hydroxychloroquine drugs on these selected zigzag nanotubes. Besides, recovery time was also explored to prophesy the nature of interactions between the drug molecule and the adsorbents in both gas and water phases.

2. Computational methods

The simulations were executed using the density functional theory (DFT) depending on 6-31G** basis set[30] which was performed in Gaussian 09 software package [31]. The 6-31G** levels basis set depending on M062X procedure were chosen according to its accuracy in electronic and structural properties especially for nanomaterials [32,33]. The vibrational frequencies were also analyzed to inspect the true global lowest level of the predicted Al-CNT, Si-CNT, and (SiC-NT).
Then, the Hydroxychloroquine drug was adsorbed on these three nanoparticles and the chemical properties including charge transfer analysis, adsorption energies, dipole moment, energy gap, and recovery time were calculated to estimate the interaction between the drug molecule to nanoparticles.
To prophesy the chemical structural stability of the adsorbents and the adsorption energy was calculated using the equations below: [34,36]. One of the quantum chemical descriptors of hardness (η) is defined as the half of the energy gap between highest occupied molecular orbital (HOMO) and the lowest unoccupied molecular orbital (LUMO) that:

$$\eta \cong \frac{1}{2}\,(E_{LUMO} - E_{HOMO}) \cong \frac{1}{2}\,(I - A) \quad (1)$$

A and I are known as the affinity of electrons and the ionization potential of the compounds.
Softness (S) can be calculated from hardness (η) and hard soft acid-base (HSAB) principle is:

$$S = \frac{1}{\eta} \quad (2)$$

Electronegativity was calculated from E_{HOMO}, E_{LUMO} by executing the Equation:

$$\chi = -\frac{1}{2}\,(E_{HOMO} + E_{LUMO}) \quad (3)$$

To calculate the effect of Hydroxychloroquine on the energies of Fermi levels and the work functions of the nanotube, Fermi levels energy were calculated by using the equation from electronegativity, Fermi energy can be estimated that Ef = -χ

$$E_f = E_{\mathrm{HOMO}} + \frac{(E_{LUMO} - E_{HOMO})}{2} \quad (4)$$

Several calculations were executed to calculate the total energies of the molecules depending on the position of the nanotube attached to the drug molecule. The adsorption energies of drug on the surfaces of the nanotubes were obtained by:

$$E_{ads} = E_{complex} - \left(E_{nanotube} + E_{drug}\right) \quad (5)$$

where $E_{complex}$, $E_{nanotube}$ and E_{drug} donate the energy of complex composed with nanotube –drug and isolated energies of nanotube and drug, respectively. The E_{ads} energy was determined from the

summation of interaction energy (E_{int}) and deformation energies (E_{def}) of drug ($E_{def\text{-}drug}$) and nanotubes ($E_{def\text{-}nanotube}$) during the adsorption process.

$$E_{int} = E_{complex} - \left(E_{nanotube\ in\ complex} + E_{drug\ in\ complex}\right) \quad (6)$$

$$E_{def} = \left(E_{drug\ in\ complex} - E_{drug}\right) + \left(E_{nanotub\ in\ complex} - E_{nanotube}\right) \quad (7)$$

where $E_{nanotube\ in\ complex}$, $E_{drug\ in\ complex}$ are the energies of nanotube and drug with their geometries in the complex, respectively.

The thermodynamical parameters were also investigated like entropy (ΔS), the change of Gibbs free energy (ΔG), and enthalpy (ΔH), to examine the structural stability by the following equations was used [37]:

$$\Delta G = G_{complex} - G_{nanotube} - G_{drug} \quad (8)$$

$$\Delta H = H_{complex} - H_{nanotube} - H_{drug} \quad (9)$$

$$\Delta S = \frac{\Delta H - \Delta G}{T} \quad (10)$$

where $H_{complex}$ and $G_{complex}$ are enthalpy and gibbs free energy of drug adsorbed onto nanotubes, G_{nano} and H_{nano} are the Gibbs free energy and enthalpy of the nanotubes and H_{drug} and G_{drug} are the enthalpy and gibbs free energy of the drug respectively, T is the room temperature which is equal to 298.15 K.

3. Results and discussions

Three nanotubes, (Al-CNT, Si-CNT, and silicon carbide (SiC-NT)) were considered for ($C_{18}H_{26}ClN_3O$) COVID-19 as drug delivery vehicles.

At first, the nanotubes and (Hydroxychloroquine) molecule were formed using DFT calculations in the gas phase. Figure 1 shows the formed geometries of the investigated nanotubes and drug molecules with their resultant HOMO, LUMO, and figure 2 illustrate the MEP for the investigated drug complex with the nanoparticles before binding.

Compound	Optimized Geometry	HOMO	LUMO
Drug complex	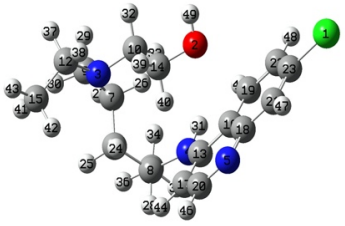	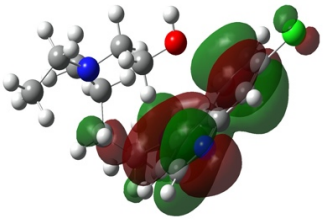	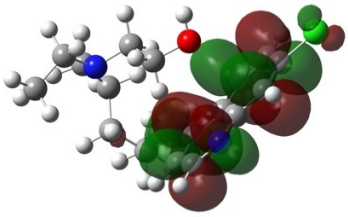
Al-CNT	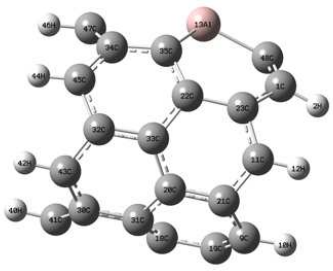	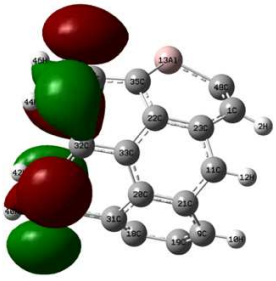	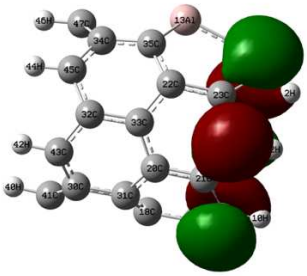

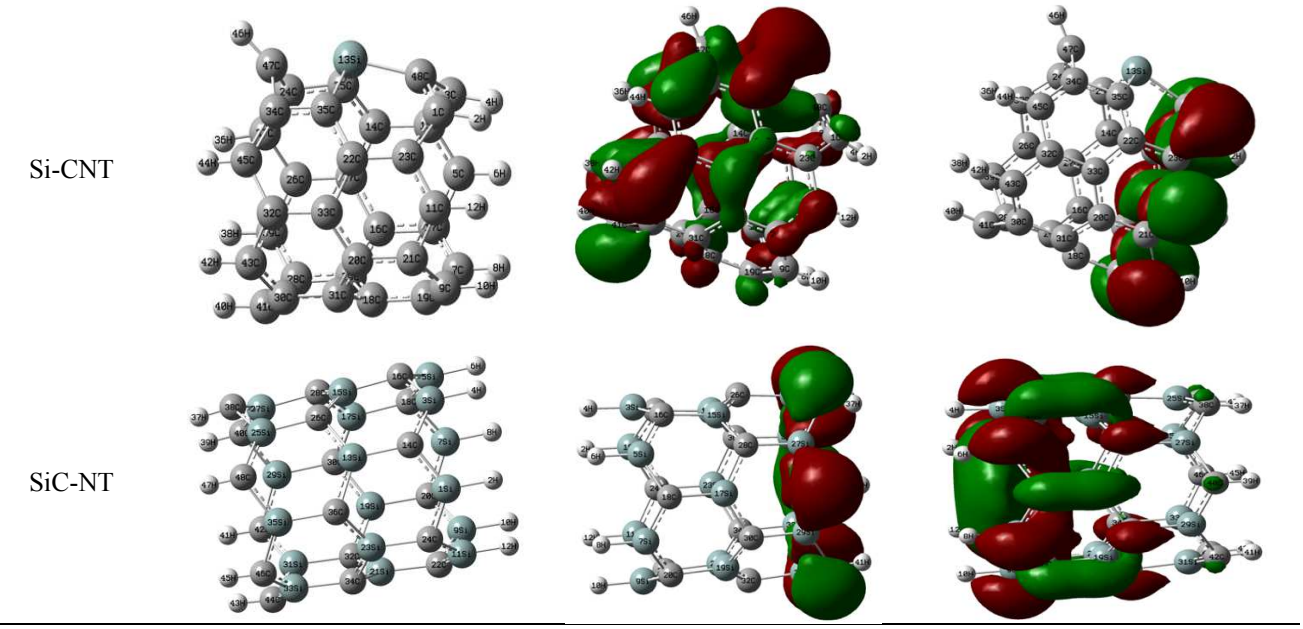

Figure1. Formed structures, HOMO, LUMO for Hydroxychloroquine, Al-CNT, Si-CNT, and SiC-NT.

Compound	Optimized Geometry	MEP
Drug complex	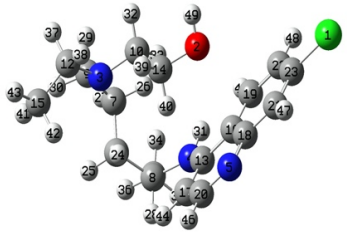	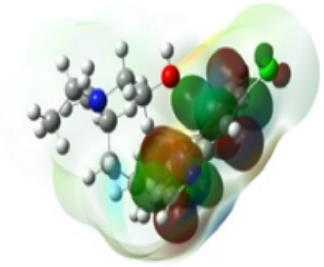
Al-CNT	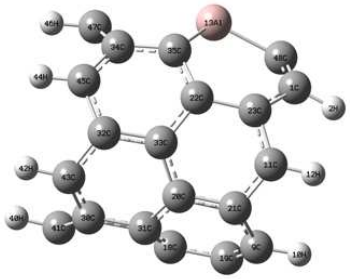	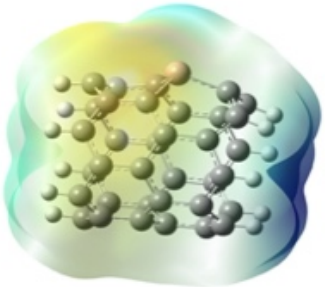
Si-CNT		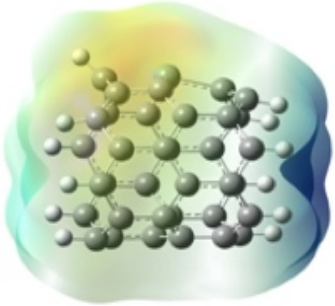

SiC-NT

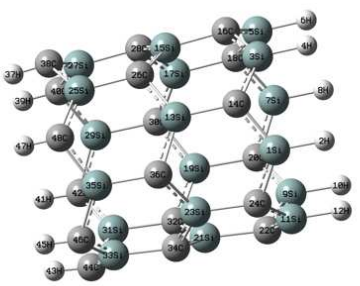

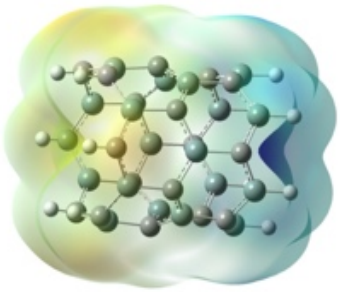

Figure2 Molecular electrostatic potential (MEP) map for Hydroxychloroquine, Al-CNT, Si-CNT, and SiC-NT. The red to blue (-0.01 a.u. to 0.01 a.u.) color scheme for MEP surface describes the electron (rich/ insufficient) region of the structure's surface respectively.

The vibrational modes of the nano-structures and the drug molecule were examined to verify the stability of the structure in the existence of IR. All of the nanotubes vibrational modes had in a positive frequency range of (99.08 to 3216.86) cm^{-1} for Al-CNT and in the range of (128.48 to 3210.06) cm^{-1} for Si-CNT, and (57.05 to 3167.20) cm^{-1} for SiC-NT.

Furthermore, the HOMO and LUMO energies were also investigated to calculate the energy gap of the nanotubes. For Al-CNT, the HOMO levels were existed on C–C bonds over one side of the nanotube, whereas LUMO levels exist on the C–C bonds opposite side of the nanotube. In the case of the Si-CNT, HOMO levels were also located on one side of the nanotube, while LUMO levels were located on almost the entire nanotube. Finally, for the SiC-NT, HOMO levels were found on the entire nanotube, but LUMO was located on one side of the nanotube. The predicted energy gap of Al-CNT, Si-CNT, and SiC-NT are (2.68, 2.64, and 2.46) eV to understand the reactive location of the Hydroxychloroquine molecule with the adsorbents.

3.1. Hydroxychloroquine adsorption on Al-CNT

To find appropriate adsorbents for Hydroxychloroquine drug, different chemical properties were investigated like electronic, adsorption properties and the geometric properties, etc. of Hydroxychloroquine/Al-CNT complexes.

Initially, the Hydroxychloroquine drug molecule was adsorbed on different locations of the Al-CNT with the best adsorption in junction of aluminum atom to O, N, and Cl atoms of the Hydroxychloroquine molecule.

Regarding to Hydroxychloroquine adsorbed complex, the geometric shape of the Al-CNT remains steady and the bond lengths of C–C had a slight change approximately ~ 0.035 Å at the close adsorption site leading to a chemical interaction between Hydroxychloroquine and Al-CNT with a confirmation of the adsorption energy and a change in electronic properties analysis. Hydroxychloroquine drug molecule was adsorbed on the Al-CNT with adsorption energy values (-45.98, -15.78, -45.15, and -93.53) kcal/mol at the minimum distance of 2.4 Å at the 6-31G** level of theory as mentioned in Table1.

Table 1. In gas phase, the adsorption energy (E_{ads}) for the new complexes (kcal/mol), (d) is the minimum distance (Å) between the Hydroxychloroquine molecule, and the adsorbents, dipole moment DM (Debye), and the recovery time τ (in seconds). The recovery time was calculated in UV light under vacuumed conditions using a frequency of 3×10^{16} sec^{-1}. at room temperature.

structure	distance (d)	dipole moment (DM)	recovery time (τ) in seconds	adsorption energy (E_{ads})
Hydroxy/Al(O)	1.90	19.04	$2.93*10^{16}$	-45.07
Hydroxy/Al(Cl)	2.45	10.88	$1.19*10^{-5}$	-15.78

Hydroxy/Al(N)	2.06	12.83	$3.75*10^{16}$	-45.15
Hydroxy/Al(N)	1.84	12.49	$9.72*10^{19}$	-93.53
Hydroxy/Si(O)	1.92	30.36	4.38	-23.38
Hydroxy/Si(Cl)	4.21	8.15	$8.07*10^{-7}$	-14.18
Hydroxy/Si(N)	2.04	17.99	24.9	-24.41
Hydroxy/Si(N)	2.04	18.15	$1.59*10^{-5}$	-15.95
Hydroxy/SiC(O)	1.95	17.96	$4.44*10^{3}$	-27.49
Hydroxy/SiC(Cl)	2.35	60.81	$7.33*10^{18}$	-48.28
Hydroxy/SiC(N)	2.15	68.26	1.52	-22.75
Hydroxy/SiC(N)	2.37	87.34	$2.06*10^{-4}$	-17.47

In the case of the Hydroxychloroquine /Al-CNT structure, the electronic parameters like E_{HOMO}, E_{LUMO}, Eg, and Fermi level energies have a noticeable change.
The values of E_{HOMO} and E_{LUMO} of Al-CNT before the adsorption of molecules were (-4.83 and -2.15) eV and after adsorption of Hydroxychloroquine, (-4.10, -4.14, -4.31, -6.04) eV for HOMO and (-1.73, -1.82, -1.88, -2.20) eV for LUMO in sequential.
The Hydroxychloroquine drug molecule had a significant small effect on the HOMO / LUMO energy level except when it was combined with the nitrogen atom with the energy gap of 3.84 eV. The symmetric Frontier molecular orbital (FMO) map is shown in Fig. 3.
To understand the sensing mechanism of the nanotubes on the drug molecule, the variation of the ΔEg gap during the adsorption process is taken into account by the following equation:

$$\%\Delta Eg = 100x(\Delta Eg2 - \Delta Eg1)/\Delta Eg1 \quad (11)$$

Where ΔEg1 and ΔEg2 are the ΔEg values of pristine NTs and complex, respectively.
Chemical sensors are related to the difference of the electrical conductance after absorbing the drug on the electron exchange between the drug and sensor. Therefore, the sensitivity of the drug on NTs is based on HOMO and LUMO energies.

Table 2. HOMO energy (E_{HOMO}) eV, LUMO energy (E_{LUMO}) eV, HOMO/LUMO energy gap (Eg), Fermi energy (EF) eV, hardness, softness, and Φ of the complexes. %Δ Eg and %ΔΦ represent the percentage of bandgap and work function of the complex with respect to the studied NTs, respectively.

	Structures	E_{HOMO} (eV)	E_{LUMO} (eV)	Energy gap (ΔEg)	%ΔEg	Fermi level (E_f) (eV)	Hardness (η)	Softness (S)	Φ	%ΔΦ
-	Hydroxy-	-6.80	-0.11	6.69	-	-3.45	3.34	0.29	3.45	-
-	Al-CNT	-4.83	-2.15	2.68	-	-3.49	1.34	0.74	3.49	-
-	Si-CNT	-4.94	-2.30	2.64	-	-3.62	1.32	0.75	3.62	-
-	SiC-NT	-5.42	-2.95	2.46	-	-4.18	1.23	0.81	4.18	-
1	Hydroxy/Al(O)	-4.10	-1.73	2.37	-11.38	-2.91	1.18	0.84	2.91	-16.53
2	Hydroxy/Al(Cl)	-4.14	-1.82	2.32	-13.16	-2.98	1.16	0.85	2.98	-14.67
3	Hydroxy/Al(N)	-4.31	-1.88	2.42	-9.63	-3.09	1.21	0.82	3.09	-11.38
4	Hydroxy/Al(N)	-6.04	-2.20	3.84	43.32	-4.12	1.92	0.52	4.12	17.93
5	Hydroxy/Si(O)	-4.14	-1.86	2.28	-13.83	-3.00	1.14	0.87	3.00	-17.14
6	Hydroxy/Si(Cl)	-4.85	-2.03	2.82	6.84	-3.44	1.41	0.70	3.44	-4.97
7	Hydroxy/Si(N)	-4.15	-1.85	2.29	-13.26	-3.19	1.14	0.87	3.19	-17.08
8	Hydroxy/Si(N)	-4.25	-1.93	2.31	-12.36	-3.09	1.15	0.86	3.09	-14.57
9	Hydroxy/SiC(O)	-5.01	-2.54	2.46	0.08	-3.78	1.23	0.80	3.78	-9.72
10	Hydroxy/SiC(Cl)	-4.78	-2.17	2.61	5.79	-3.47	1.30	0.76	3.47	-16.93
11	Hydroxy/SiC(N)	-5.01	-2.75	2.26	-8.39	-3.88	1.13	0.88	3.88	-7.14
12	Hydroxy/SiC(N)	-5.75	-3.18	2.57	4.25	-4.47	1.28	0.77	4.47	6.76

The calculated results for the hardness showed that the new compounds became less hard than the original drug compound, where the highest value was obtained when the drug compound was bonded with (Al-CNT) through the nitrogen atom and the value of (1.92), on the other hand, the highest value of softness was obtained when the drug compound was bonded With (SiC-NT) through the nitrogen atom as well with a value of (0.88), and this confirms the superiority of (Al-CNT) in bonding with the drug compound, excluding the rest of the nanoparticles used[38].
On the other hand, the calculated results for the value of the Fermi energies varied according to the type of nanoparticle used, but it was noticed that the value of the Fermi energy when using (Al-CNT) through the nitrogen atom has increased significantly than the rest of the other new compounds and the value of (4.12) eV, which confirms the occurrence of a stronger bond of this complex is better from the others new complexes[39].
The percentage change values of ΔEg for each complex are given in Table2. As reported energies of E_{HOMO} and E_{LUMO} and energy gap (ΔEg), the electronic properties of all studied NTs were affected by the adsorption of the Hydroxychloroquine drug. The decreasing order of percentage change values is obtained for complex1, complex2, complex3, complex5, complex7, complex8, and complex 11 while increasing is for other complexes. The highest increased percentage value of %43.32 is calculated for complex4 which has the largest minimum adsorption energy (-93.53 kcal/mol) in Table 1.
The other calculated quantity is the work function required to remove single electron from Fermi level is calculated by the variation of the work function during the adsorption process is defined as ΔΦ. The percentage value of %ΔΦ can be deduced as the percentage value of %ΔEg using the Eq. (11). The calculated percentage values of ΔΦ for each complex are also given in Table 2. It is clear that the highest value is obtained for complex4 with a value of %17,92. As a result, the values given in Table 2 show that complex 4 can be used as an amperometric sensor to detect the Hydroxychloroquine drug molecule.

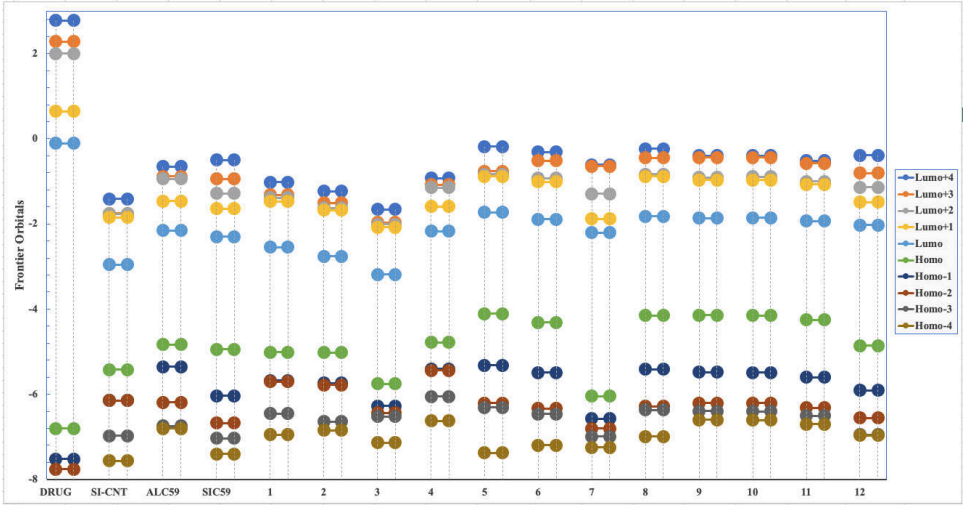

Figure 3. Energy gap between HOMO and LUMO for Hydroxychloroquine drug , Si-CNT, Al-CNT, and SiC-NT, with all investigated location regarding to the position of the nanotube ((1) Hydroxy/Al-CNT (O), (2) Hydroxy/Al-CNT (Cl) (3) Hydroxy/Al-CNT(N) (4) Hydroxy/Al-CNT(N), (5)Hydroxy/Si-CNT(O), (6) Hydroxy/Si-CNT(Cl), (7) Hydroxy/Si-CNT(N), (8)Hydroxy/Si-CNT(N), (9) Hydroxy/SiC-NT(O), (10) Hydroxy/SiC-NT(Cl), (11) Hydroxy/SiC-NT(N), (12) Hydroxy/SiC-NT(N)

To comprehend the charge transferring between the drug molecules and nanotubes, and to envisage charge density distribution around the complexes, the electrostatic potential map of the molecules

was inspected. The MEP map illustrates the nucleophilic (positive) region pointed by the blue color and the electrophilic (negative) region pointed by the red region and the neutral region of the complexes. Figures 1 and 4 are shown the MEP of the drug molecule by suggesting nanotubes and their complexes.

For the Hydroxychloroquine drug molecule, electron densities were highly concentrated around O and N atoms, and for the Al-CNT, positive, negative, and neutral regions were regularly distributed throughout the whole tube where electron distribution was found around C–C bonds, and the electron lack was found at the hexagonal and pentagonal rings.

After Hydroxychloroquine molecule was adsorbed on the Al-CNT, the electron-deficient (blue) region on the Hydroxychloroquine molecule was less than before causing the molecule to get a neutral (white) region which means the charge transfer from the nanoparticles to the drug molecule.

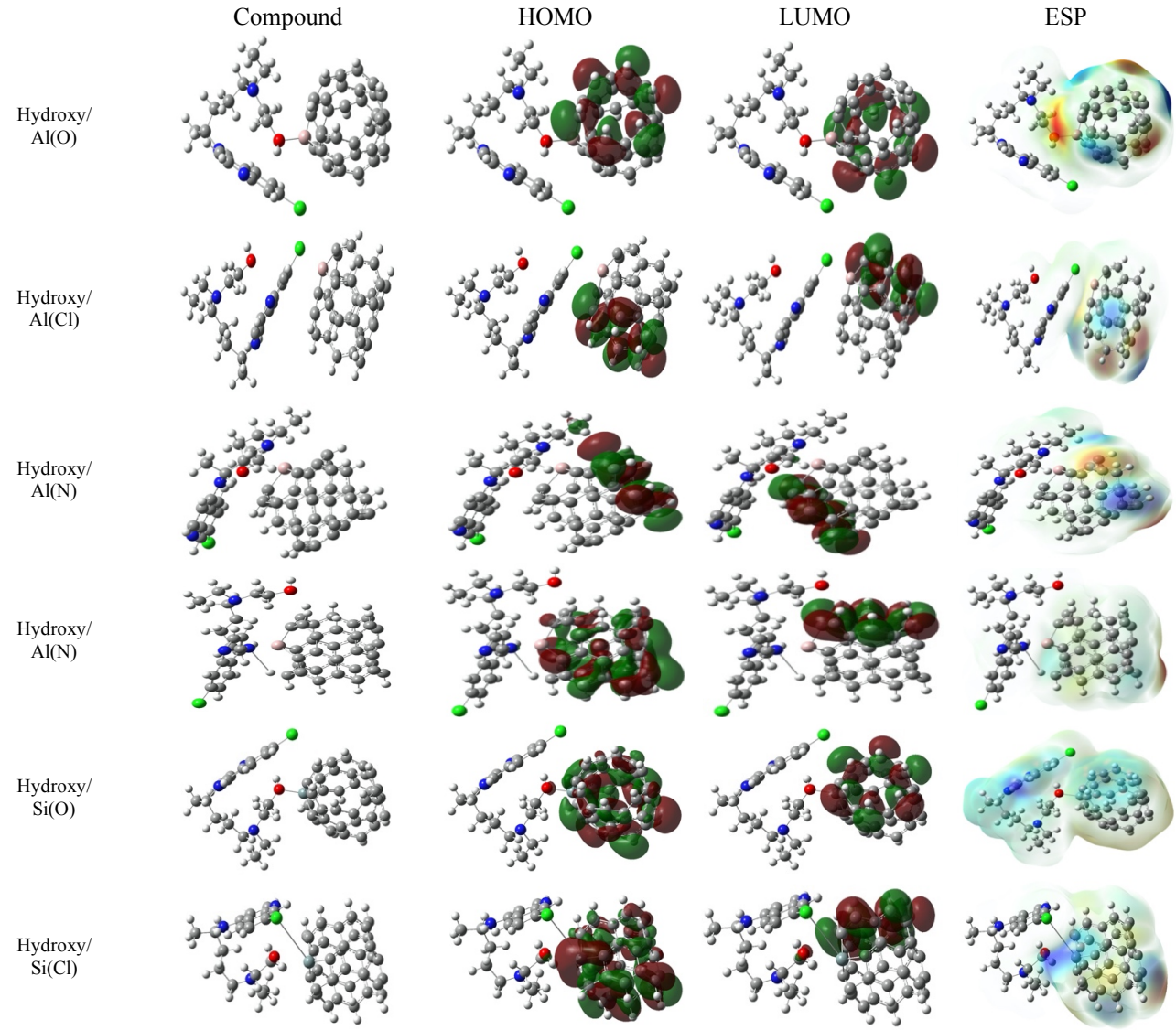

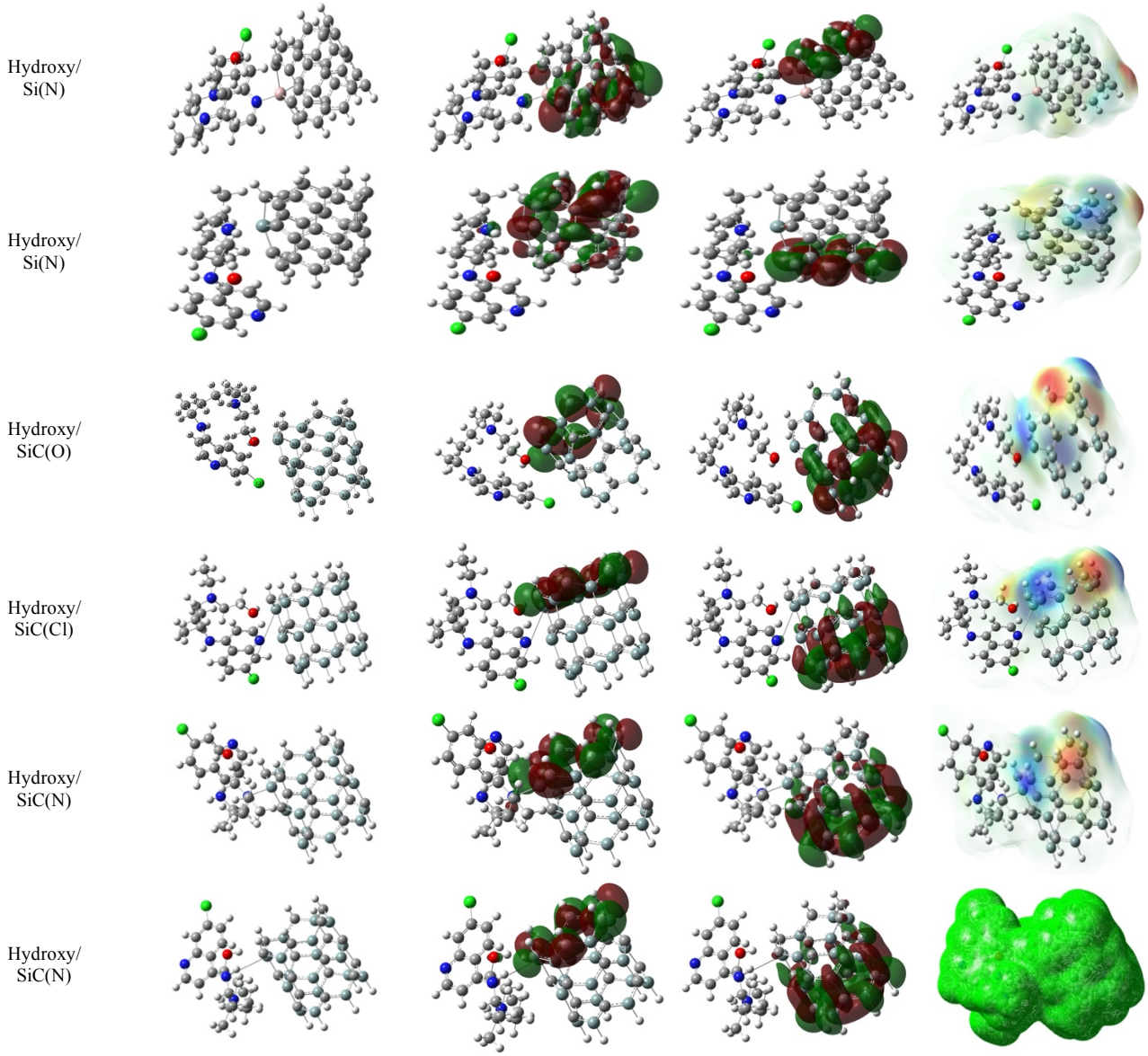

Figure 4. Frontier molecular orbital (HOMO and LUMO) for all investigated complexes. The given iso value is 0.02 electron/bohr3.

Recovery time (desorption time) is the value of time desired for the drug to be desorbed from the adsorbents with a significant parameter that is used for sensors and drug delivery systems. This parameter is directly connected to the energy of adsorption, where the high adsorption interaction requires a high desorption time and vice versa.
Recovery time (τ) is calculated using the equation [40]:

$$\tau = \frac{1}{\nu} Exp(\frac{-E_{ads}}{kT}) \quad (12)$$

Where T, K, and ϑ are the temperature, Boltzmann's constant and the attempted frequency, respectively. (~2×10^{-3} kcal/mol K).

Hydroxychloroquine molecule seems to be adsorbed on the Al-CNT with high adsorption energies; a different recovery time (table 1) was obtained under the conditions of UV light with frequency $\nu \sim 3*10^{16}$ s^{-1} at room temperature.
Thus, a small distance between the adsorbate and the adsorbent, with high adsorption energy and a large value of charge transfer from the nanotube to Hydroxychloroquine drug molecule demonstrates that Al-CNT is suitable for Hydroxychloroquine drug carrier.
The values varied between the active atoms in the new complexes, and the greatest amount was found through combination the nanotube with the Hydroxychloroquine molecule through the nitrogen atom.

3.2. Hydroxychloroquine adsorption on Si-CNT

To investigate further properties of different nanostructures with the drug molecule, the previous nanotube Al-CNT was replaced with the Si-CNT. The optimized Si-CNT shows good stability of the structure which was confirmed by calculating the energy.
Four different locations on the drug depend on the active atoms (O, Cl, N,N) which were confirmed to be more stable site of adsorption for the Hydroxychloroquine molecule. The Hydroxychloroquine drug molecule was adsorbed at (1.92, 2.21, 2.04, 2.04). Å distance on the surface of Si-CNT with adsorption energies (-23.38, -14.18, -24.41, -15.95) kcal/mol on (O, Cl, N,N) atoms respectively using the 6-31G** basis set.
From the adsorption energy values, there was a noticeable interaction between Hydroxychloroquine and Si-CNT in a physisorption range [41]. The bond length at the adsorption position before and after adsorption of the Hydroxychloroquine drug is mentioned in table 4. Thus, Hydroxychloroquine drug slightly distorted the geometry of Si-CNT which implies a slight interaction between Hydroxychloroquine and this nanotube. For the Si-CNT, there was another change in the values of HOMO, LUMO, and Energy gap (table 2), and also a slight change in energy gap after the adsorption.
Similarly, the energy gap of Hydroxychloroquine has a variation after adsorption between the drug and the nanoparticles; therefore, the change in energy gap is responsible for the interaction between the drug and the nanoparticles. Because of the weak values of E_{ads}, Si-CNT is not suitable to be used as a drug delivery vehicle regarding Hydroxychloroquine drug. MEP map shows that the most amount of charge was located on the nanotube except in the case of combining with the oxygen atom.
Unlike Hydroxychloroquine drug adsorption on the Al-CNT, the recovery time has been found for the Si-CNT to be very short except in the case when the nanotube was added to the nitrogen atom, where the recovery time was (24.9) sec, which can be considered as an acceptable value to desorb drug from Si-CNT surface by comparing with those obtained for other locations of complex/Si-CNT.
All the information regarding the adsorption properties of the drug over the Si-CNT was mentioned in table 1.

3.3. Hydroxychloroquine adsorption on SiC-NT

In order to enclose all the circumstances surrounding the chemical properties, another nanoparticle, SiC-NT , was introduced to Hydroxychloroquine drug.
The Hydroxychloroquine drug molecule was adsorbed on the optimized SiC-NT and it prefers to be adsorbed again at the active atoms on the drug (O, Cl, N, N) where the atoms of the

Hydroxychloroquine molecule gets close to the nanotube with a minimum adsorption distance of (1.95, 2.35, 2.15, 2.37) Å.
The Hydroxychloroquine drug molecule was adsorbed on the optimized SiC-NT on the preferred active atoms on the drug (O, Cl, N, N) where the atoms of the Hydroxychloroquine molecule gets close to the nanotube with a minimum adsorption distance of (1.95, 2.35, 2.15, 2.37)Å.
So, there was an interaction between the Si atom of SiC-NT and the active atoms of the Hydroxychloroquine drug molecule through the adsorption process.
In the Hydroxychloroquine/SIC-NT complex, there was no change in the bond lengths at the close adsorption site of the SiC-NT. The calculated adsorption energy was found to be (-48.28, -22.75, -17.47) kcal/mol for the investigated frequency. In Si-CNT, the values of absorbance energy were not enough to consider this nanoparticle as a suitable drug delivery vehicle, and the recovery time obtained was much larger than other nanotubes used as shown in table1.
The electronic properties of SiC-NT were significantly affected by the adsorption of Hydroxychloroquine drug molecules. For Hydroxychloroquine/SiC-NT complex, the HOMO and LUMO energies of SiC-NT had a slight shift from other nanotubes (Table2).
Consequently, the HOMO and LUMO levels became unstable after the adsorption of the Hydroxychloroquine molecule on the SiC-NT. At the same time, Fermi energy levels, energy gap, and work function before and after the Hydroxychloroquine drug molecule adsorption changed.
The total density of states (TDOS) and PDOS, OPDOS diagrams of the complex structure of Hydroxychloroquine compounds interacting with Al-CNT was selected to plot in Figure 5 because the significant %ΔEg values are given in Table 2, each was also calculated to better understanding the stability of system. The change in Eg by DOS analysis can be confirmed as shown in Figure 5 by the MULTIWFN program [42].

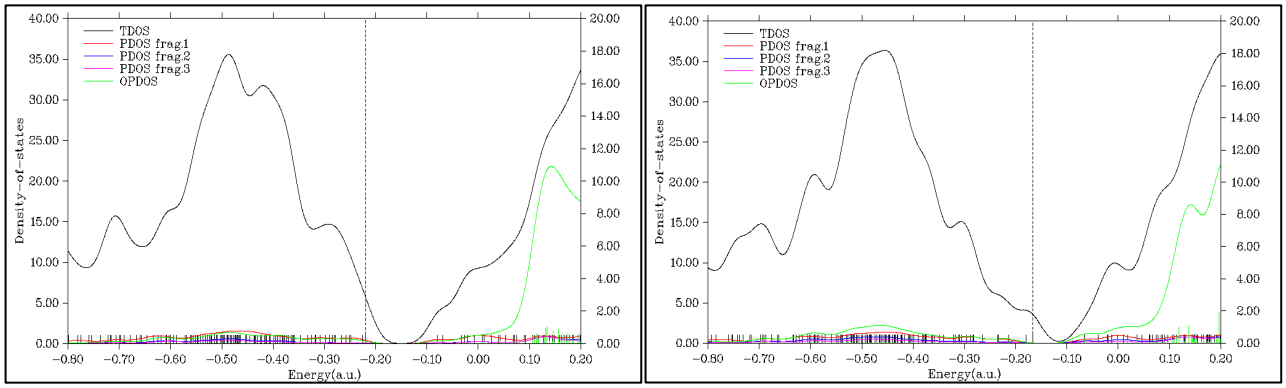

Figure 5. TDOS and PDOS plots for complex structure of N-BMSF-BENZ /Al-CNT. The dashed line shows the HOMO energy level. Where frag. 1 (CNT), frag.2 (Hydroxychloroquine) drug, frag. 3 (Hydroxychloroquine/CNT complexes)

The stability of the complex's thermodynamic properties, thermodynamic parameters, Gibbs free energy (ΔG), the change in enthalpy (ΔH), and entropy (ΔS) were evaluated by equations (9–11) and the values were mentioned in Table 3. Positive values of ΔH and ΔG indicate that the reaction has an exothermic and spontaneous processes, and vice versa[43].

Table 3. (ΔG) Gibbs free energy (kcal/mol), (ΔH) enthalpy (kcal/mol), (ΔS) entropy (kcal/mol.K), the minimum and the maximum frequencies (cm^{-1}) for the different complex at gas phase.

	Structure	ΔG	ΔH	ΔS	Vmin	Vmax
-	Hydroxy-	-	-	-	18.21	3819.36

-	Al-CNT	-	-	-	99.08	3216.86
-	Si-CNT	-	-	-	128.48	3210.06
-	SiC-NT	-	-	-	57.05	3167.20
1	Hydroxy/Al(O)	-2.51	-25.55	-0.04	14.63	3717.25
2	Hydroxy/Al(Cl)	-5.49	-17.23	-0.03	8.08	3815.80
3	Hydroxy/Al(N)	-43.32	-60.04	-0.05	13.18	3820.02
4	Hydroxy/Al(N)	-24.97	-26.19	-0.05	10.10	3817.20
5	Hydroxy/Si(O)	-14.03	-27.32	-0.04	9.60	3664.50
6	Hydroxy/Si(Cl)	-2.008	36.87	0.13	13.55	3706.77
7	Hydroxy/Si(N)	-25.73	-43.37	-0.05	12.57	3803.40
8	Hydroxy/Si(N)	-18.80	-35.24	-0.05	13.92	3812.99
9	Hydroxy/SiC(O)	-19.39	-34.19	-0.04	11.81	3673.18
10	Hydroxy/SiC(Cl)	-57.07	-71.49	-0.04	13.73	3653.35
11	Hydroxy/SiC(N)	-24.55	-42.77	-0.06	11.81	3777.66
12	Hydroxy/SiC(N)	-5.47	-21.45	-0.05	-6.83	3700.08

The calculated values of ΔH and ΔG were negative for all new complexes at all investigated nanotubes, meaning these new complexes were exothermic and spontaneous.
ΔS with negative values indicate that the complex is ordered [44]. That's why the thermodynamic parameters show that the investigated nanotubes are more appropriate by evaluating the thermodynamic stability for Hydroxychloroquine drug delivery.
As a method to ensure structural stability, and by using a specific infrared (IR) spectroscopy on the studied Hydroxy/CNT complexes, the results of the frequencies of the new complexes showed that the frequency range has changed from (3819.36) cm^{-1} in the case of hydroxychloroquine to varying values ranging between (3653.35) cm^{-1} as a minimum and (3820.02) cm^{-1} as a maximum value (table 3), where this value was recorded at the complex (Hydroxy/Al-CNT(N)), which proves that the intensity of the frequencies has changed to higher values than it was, and therefore these values indicate an acceptable interaction intensity between the nanoparticles and the drug compound, especially when the interaction between the drug compound and (Al-CNT) was at the nitrogen atom.[45]
On the other hand, the positive values of the vibrations indicate that the reaction is stable with minimal waste energy.[45]

3.4 Aqueous solution effect

The results of aqueous solution were researched understanding the importance the real environment for the adsorbate-adsorbent complexes. More optimization for only stable complexes in water was done with the same methods.
Once more, adsorption energy, E_{HOMO} and E_{LUMO} energies, energy gap, dipole moment, etc. were calculated using the same equations illustrated in the computational section. It was noticed that all adsorption energies had negative values just like the gas phase leading to confirm that there is an exothermic and attractive reaction happen in the water media. A weak interaction was measured between the Hydroxychloroquine drug and the Si-CNT and SiC-NT confirmed by the adsorption energies (table 5). Fig. 6 clarifies the bar diagram of adsorption energy in the gas and water phases.

Table 4. Bond length between active atoms of the nanotubes before and after adsorption of Hydroxychloroquine drug in gas and water phases

Structure	Bond location	Bond before adsorption	Bond after adsorption/ Gas phase	Bond after adsorption/ Water phase	Nanoparticle structure
Al/Hydroxy(O)	Al-C25	1.88	1.91	1.91	

	Al-C35	1.88	1.91	1.92	
	Al-C45	1.88	1.91	1.92	
	Al-C25	1.88	1.90	1.90	
Al/Hydroxy(Cl)	Al-C35	1.88	1.90	1.91	
	Al-C45	1.88	1.90	1.90	
	Al-C25	1.88	1.93	1.93	
Al/Hydroxy(N)	Al-C35	1.88	1.92	1.94	
	Al-C45	1.88	1.92	1.93	
	Al-C25	1.88	1.99	1.94	
Al/Hydroxy(N)	Al-C35	1.88	1.99	1.99	
	Al-C45	1.88	1.99	1.99	
	Si-C25	1.88	1.92	1.92	
Si/Hydroxy(O)	Si-C35	2.07	1.84	1.84	
	Si-C45	1.83	1.84	1.85	
	Si-C25	1.88	1.87	1.87	
Si/Hydroxy(Cl)	Si-C35	2.07	1.84	1.83	
	Si-C45	1.83	1.83	1.84	
	Si-C25	1.88	1.93	1.94	
Si/Hydroxy(N)	Si-C35	2.07	1.85	1.86	
	Si-C45	1.83	1.85	1.86	
	Si-C25	1.88	1.92	1.92	
Si/Hydroxy(N)	Si-C35	2.07	1.85	1.85	
	Si-C45	1.83	1.84	1.85	
	Si-C14	1.76	1.76	1.76	
SiC/Hydroxy(O)	Si-C16	1.76	1.76	1.76	
	Si-H4	1.4	1.4	1.47	
	Si-C14	1.76	1.75	1.76	
SiC/Hydroxy(Cl)	Si-C16	1.76	1.76	1.76	
	Si-H4	1.4	1.4	1.47	
	Si-C14	1.76	1.76	1.76	
SiC/Hydroxy(N)	Si-C16	1.76	1.76	1.76	
	Si-H4	1.4	1.4	1.47	
	Si-C14	1.76	1.76	1.76	
SiC/Hydroxy(N)	Si-C16	1.76	1.76	1.76	
	Si-H4	1.4	1.4	1.47	

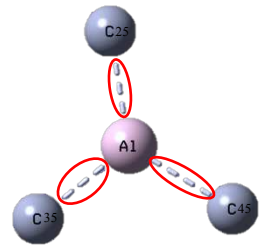

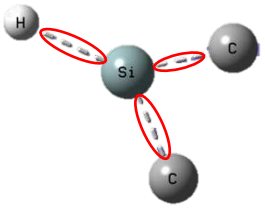

Table 5. In water phase, the adsorption energy (E_{ads}) for the new complexes in (eV), (d) is the minimum distance (Å) between the Hydroxychloroquine molecule, and the adsorbents, dipole moment DM (Debye), and the recovery time τ (sec). The recovery time was calculated in UV light under vacuumed conditions using a frequency of 3×10^{16} s^{-1} at room temperature.

Structure	Distance (d) In Å	Dipole Moment (DM) In Debye	Recovery time (τ) In seconds	Adsorption energy (E_{ads}) In eV

Hydroxy-	-	11.94	-	-
Al-CNT	-	9.30	-	-
Si-CNT	-	126.20	-	-
SiC-NT	-	13.30	-	-
Hydroxy/Al(O)	1.88	46.53	$1.64*10^{-06}$	-43.02
Hydroxy/ Al(Cl)	2.42	21.41	$1.92*10^{17}$	-14.43
Hydroxy/Al(N)	2.04	33.46	$3.45*10^{19}$	-43.86
Hydroxy/Al(N)	1.86	25.68	47.79	-88.97
Hydroxy/Si(O)	1.89	75.26	$6.37*10^{-10}$	-24.01
Hydroxy/Si(Cl)	4.51	16.69	14921.06	-9.14
Hydroxy/Si(N)	2.002	48.53	$2.04*10^{-05}$	-25.66
Hydroxy/Si(N)	2.007	44.54	$3.33*10^{-17}$	-14.77
Hydroxy/SiC(O)	1.95	68.51	$1.73*10^{18}$	-22.48
Hydroxy/SiC(Cl)	2.35	185.22	2.04692	-45.25
Hydroxy/SiC(N)	2.08	223.89	$1.21*10^{-06}$	-21.08
Hydroxy/SiC(N)	4.27	241.51	$1.19*10^{16}$	-13.38

The negative value of adsorption energies in water shows an attractive and exothermic reaction occurs. The change in adsorption energy is:

$$\Delta E_{Sol.-gas} = E_{ads}(water) - E_{ads}(gas) \quad (13)$$

where $\Delta E_{Sol\text{-}gas}$ is the difference between the adsorption energy of drug adsorbed complexes in the gas and water phase. Values of $\Delta E_{Sol\text{-}gas}$ are mentioned in table 6.

Table 6. $\Delta E_{Sol\text{-}gas}$ for all investigated complexes in kcal/mol

	Structure	E_{ads} Gas phase	E_{ads} Water phase	$\Delta E_{Sol\text{-}gas}$
1	Hydroxy/Al(O)	-45.006	-43.028	1.977
2	Hydroxy/Al(Cl)	-15.783	-14.437	1.346
3	Hydroxy/Al(N)	-45.153	-43.866	4.555
4	Hydroxy/Al(N)	-93.534	-88.978	1.286
5	Hydroxy/Si(O)	-23.387	-24.016	-0.628
6	Hydroxy/Si(Cl)	-14.184	-9.148	5.035
7	Hydroxy/Si(N)	-24.418	-25.660	-1.241
8	Hydroxy/Si(N)	-15.953	-14.775	1.177
9	Hydroxy/SiC(O)	-27.493	-22.488	5.005
10	Hydroxy/SiC(Cl)	-48.283	-45.256	3.026
11	Hydroxy/SiC(N)	-22.757	-21.087	1.670
12	Hydroxy/SiC(N)	-17.476	-13.387	4.088

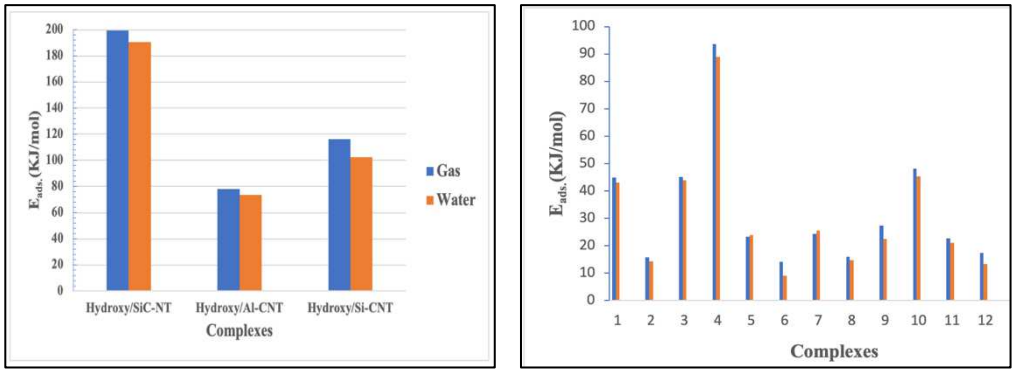

Fig. 6. A comparison between the adsorption energy of the new complexes in the gas and water phases.
A. (1).Hydroxy/Al-CNT(O), (2).Hydroxy/Al-CNT (Cl) (3).Hydroxy/Al-CNT(N) (4).Hydroxy/Al-CNT(N), (5).Hydroxy/Si-CNT(O), (6).Hydroxy/Si-CNT(Cl), (7).Hydroxy/Si-CNT(N), (8).Hydroxy/Si-CNT(N), (9).Hydroxy/SiC-NT(O), (10).Hydroxy/SiC-NT(Cl), (11).Hydroxy/SiC-NT(N), (12).Hydroxy/SiC-NT(N)
B. Over all energy deference between gas and water phase for all investigated complexes.

Thus, the adsorption energies for Hydroxy/SiC-NT, Hydroxy/Al-CNT, and Hydroxy/Si-CNT in water have fewer negative values than in the gas phase. It was noticed that only in combining the Si-CNT with the drug in (N, and O), the energy was much that we got in the gas phase.
The percentage changes in values for %ΔEg of each complex and the values of energies of E_{HOMO} and E_{LUMO} and energy gap (Eg) were given in Table 7.
The electronic properties of all studied NTs were affected by the adsorption of the Hydroxychloroquine drug. The decreasing order of percentage change values is obtained for Hydroxy/Al-CNT(N), Hydroxy/Si-CNT(O), Hydroxy/Si-CNT(N), Hydroxy/Si-CNT(N), Hydroxy/SiC-NT(O), Hydroxy/SiC-NT(Cl), Hydroxy/SiC-NT(N) complexes, while increasing for other complexes. The highest increased percentage value is calculated for Hydroxy/Al-CNT(N), which has the largest minimum absorption energy -0.15 kcal/mol.

Table 7. HOMO energy (E_{HOMO}) eV, LUMO energy (E_{LUMO}) eV, HOMO/LUMO energy gap (Eg), Fermi energy (EF) eV, Hardness, Softness, and Φ of the investigated complexes. %Δ Eg and %ΔΦ represent the percentage of bandgap and work function of the complex with respect to the studied NTs, respectively.

Structures	E_{HOMO} (eV)	E_{LUMO} (eV)	Energy gap (ΔEg)	%ΔEg	Fermi level (E_f) (eV)	Hardness (η)	Softness (S)	Φ	%ΔΦ
Hydroxy-	-7.01	-0.43	6.57	-	-3.72	3.28	0.30	3.72	-
Al-CNT	-4.97	-1.98	2.99	-	-3.48	1.49	0.66	3.48	-
Si-CNT	-5.06	-2.10	2.96	-	-3.58	1.48	0.67	3.58	-
SiC-NT	-5.85	-2.44	3.40	-	-4.15	1.70	0.58	4.15	-
Hydroxy/Al(O)	-4.86	-1.78	3.08	3.08	-3.32	1.54	0.64	3.32	-4.51
Hydroxy/Al(Cl)	-4.87	-1.86	3.00	0.45	-3.37	1.50	0.66	3.37	-5.96
Hydroxy/Al(N)	-4.81	-1.82	2.98	-0.15	-3.31	1.49	0.66	3.31	-4.63
Hydroxy/Al(N)	-5.96	-1.98	3.97	32.67	-3.97	1.98	0.50	3.97	14.20
Hydroxy/Si(O)	-4.65	-1.94	2.70	-8.69	-3.30	1.35	0.73	3.30	-7.89
Hydroxy/Si(Cl)	-5.10	-2.04	3.05	3.06	-3.57	1.52	0.65	3.57	-0.37
Hydroxy/Si(N)	-4.58	-1.94	2.63	-11.07	-3.26	1.31	0.75	3.26	-8.84
Hydroxy/Si(N)	-4.62	-1.94	2.68	-9.59	-3.28	1.34	0.74	3.28	-8.27
Hydroxy/SiC(O)	-5.59	-2.32	3.26	-4.07	-3.95	1.63	0.61	3.95	-4.70
Hydroxy/SiC(Cl)	-5.45	-2.13	3.31	-2.70	-3.79	1.65	0.60	3.79	-8.61
Hydroxy/SiC(N)	-5.37	-2.32	3.04	-10.53	-3.85	1.52	0.65	3.85	-7.19
Hydroxy/SiC(N)	-5.95	-2.48	3.47	1.90	-4.21	1.73	0.57	4.21	1.63

To check the solubility of the Hydroxychloroquine adsorbed on SiC-NT, Al-CNT, and Si-CNT complexes in the solvent, the solvation Gibbs free energy (ΔG_{Sol}) is calculated by performing the following equation [46]:

$$\Delta E_{Sol} = G_{(Drug-nano)Sol.} - (G_{(nano)Sol.} + G_{(Drug)Sol.}) \quad (14)$$

where $G_{(Drug\text{-}nanotubes)Sol}$, $G_{(nanotubes)Sol}$, and $G_{(Hydroxychloroquine\ )Sol}$ are the Gibbs free energy of the Hydroxychloroquine adsorbed complexes-adsorbents and Hydroxychloroquine drug, respectively. The values of (ΔG_{Sol}) for our studied complexes for the interaction of Hydroxychloroquine drug with Al-CNT, Si-CNT, and SiC-NT are shown in table 8.
The negative values of (ΔG_{Sol}) detect the spontaneous adsorption phenomenon, thus the adsorption of Hydroxychloroquine drug on these nanoparticles is more favorable because a spontaneous and appropriate adsorption behavior is clear.

Table 8. (ΔG) Gibbs free energy (kcal/mol), (ΔH) enthalpy (kcal/mol), (ΔS) entropy (kcal/mol.K), the minimum and the maximum frequencies (cm^{-1}), for the different complex in water phase.

Structure	ΔG	ΔH	ΔS	Vmin	Vmax
Hydroxy-	-	-	-	28.16	3806.85

Al-CNT	-	-	-	104.16	3232.90
Si-CNT	-	-	-	127.46	3222.65
SiC-NT	-	-	-	-26.13	3154.75
Hydroxy/Al(O)	-35.48	-49.32	-0.046	14.97	3692.39
Hydroxy/Al(Cl)	-4.36	-15.91	-0.038	9.89	3803.48
Hydroxy/Al(N)	-42.30	-60.03	-0.059	14.52	3802.21
Hydroxy/Al(N)	-24.81	-25.37	-0.048	12.34	3806.69
Hydroxy/Si(O)	-12.95	-29.77	-0.052	-7.01	3657.85
Hydroxy/Si(Cl)	3.42	42.26	0.130	15.65	3685.51
Hydroxy/Si(N)	-27.40	-44.93	-0.058	9.89	3776.27
Hydroxy/Si(N)	-22.36	-34.70	-0.041	6.60	3810.20
Hydroxy/SiC(O)	-14.86	-29.79	-0.050	14.13	3656.72
Hydroxy/SiC(Cl)	-55.39	-72.69	-0.058	11.23	3646.44
Hydroxy/SiC(N)	-26.04	-43.17	-0.057	11.94	3774.13
Hydroxy/SiC(N)	-30.7	-30.4	0.001	8.26	3607.09

A substantial investigation for solvent effect on the complex which is directly related to the solubility of a complex is the dipole moment property, where the high value of the dipole moment refers to the higher reactivity, conductivity, and solubility in a polar media such as water [47].
The Dipole Moment (D.M) value of Hydroxychloroquine molecule in water was 11.94, which indicates a polar molecule, and after it was adsorbed on SiC-NT, Al-CNT, and Si-CNT, the dipole moments values which were obtained in gas phase, nearly doubled in the water phase. The values of D.M are mentioned in table1 for gas phase and also in water phase (Table 5).
Once again, the results of vibration in the aqueous state showed that the values of frequencies increased in the new compounds than they were before adsorption, especially for the compound (Hydroxy/Al-CNT(N)), which proves the validity of the results in the gas state, in addition to the fact that the interaction is stable and with the lowest value of energy expended, since these frequencies came with a positive value

4. Conclusions

To predict an appropriate drug delivery method for the Hydroxychloroquine drug, an investigation was performed on the adsorption behavior of Hydroxychloroquine drug on the surface of Al-CNT, Si-CNT, and SiC-NT by using DFT calculation. It was noticed that the Hydroxychloroquine molecule was adsorbed on the surface of the nanotube with different adsorption energy depending on the closest distance between the active atom on the drug (O, Cl, N_1, and N_2), and the doped atom on the nanotube (Al, Si, and SiC).
Energies of HOMO/LUMO, energy gap, and the energies of Fermi levels had a slight change after the adsorption of the Hydroxychloroquine drug on the nanoparticles. The calculated parameters such as small charge transfer, large adsorbent-adsorbate distance, and low adsorption energy imply a weak interaction of Si-CNT and SiC-NT towards Hydroxychloroquine drug molecule MEP analysis.
Nevertheless, in the case of the Al-CNT, the Hydroxychloroquine drug prefers to be adsorbed with an adsorption energy of (-45.07, -15.78, -45.15, -93.53) kcal/mol in the gas phase, and (-43.02, -14.43, -43.86, -88.97) kcal/mol for water, which is considered more appropriate for the drug delivery system.
Likewise, Gibbs's free energy for aqueous solution evidence that Hydroxychloroquine/Al-CNT configuration shows spontaneous and appropriate adsorption in water than Hydroxychloroquine/Si-CNT and Hydroxychloroquine/SiC-NT complexes. Thus, we propose that

the Al-CNT can be a promising candidate as a drug delivery vehicle for Hydroxychloroquine drug molecules.

Reference:

1. Tönnesmann, E., Kandolf, R., & Lewalter, T. (2013). Chloroquine cardiomyopathy-a review of the literature. Immunopharmacology and Immunotoxicology, 35(3), 434–442. https://doi.org/10.3109/08923973.2013.780078.
2. Paul Hudson. (2017). Plaquenil ® Hydroxychloroquine Sulfate Tablets, USP Description. Fda. Retrieved from http://www.cdc.gov/malaria.
3. FDA. (2018). Aralen (Chloroquine Phosphate), 1–8. Retrieved from https://www.accessdata.fda.gov/drugsatfda_docs/label/2018/006002s045lbl.pdf.
4. Ben-Zvi, I., Kivity, S., Langevitz, P., & Shoenfeld, Y. (2012). Hydroxychloroquine: From malaria to autoimmunity. Clinical Reviews in Allergy and Immunology, 42(2), 145–153. https://doi.org/10.1007/s12016-010-8243-x.
5. Koranda, F. C. (1981). Antimalarials. Journal of the American Academy of Dermatology, 4(6), 650–655. https://doi.org/10.1016/S0190-9622(81)70065-3.
6. Katz, S. J., & Russell, A. S. (2011). Re-evaluation of antimalarials in treating rheumatic diseases: Re-appreciation and insights into new mechanisms of action. Current Opinion in Rheumatology, 23(3), 278–281. https://doi.org/10.1097/BOR.0b013e32834456bf.
7. Wang, L., Wang, Y., Ye, D., & Liu, Q. (2020). Review of the 2019 novel coronavirus (SARS-CoV-2) based on current evidence. *International Journal of Antimicrobial Agents*, *55*(6), 105948. https://doi.org/10.1016/j.ijantimicag.2020.105948.
8. S. Mias, J. Sudor, H. Camon, PNIPAM: A thermo-activated nano-material for use in optical devices, Microsyst. Technol. 14 (2008) 747–751, https://doi.org/10.1007/s00542007-0457-3.
9. M. Gu, Q. Zhang, S. Lamon, Nanomaterials for optical data storage, Nat. Rev. Mater. 1 (2016) 1–14, https://doi.org/10.1038/natrevmats.2016.70.
10. S.S. Varghese, S. Lonkar, K.K. Singh, S. Swaminathan, A. Abdala, Recent advances in graphene based gas sensors, Sens. Actuat., B Chem. 218 (2015) 160–183, https://doi.org/10.1016/j.snb.2015.04.062.
11. A.S. Rad, K. Ayub, Ni adsorption on Al12P12 nano-cage: A DFT study, J. Alloys Compd. 678 (2016) 317–324 https://doi.org/10.1016/j.jallcom.2016.03.175.
12. P. Pannopard, P. Khongpracha, M. Probst, J. Limtrakul, Gas sensing properties of platinum derivatives of single-walled carbon nanotubes: A DFT analysis, J. Mol. Graph. Model. 28 (2009) 62–69, https://doi.org/10.1016/j.jmgm.2009.04.005.
13. Anticancer Drug Delivery with Nanoparticles, (n.d.). http://iv.iiarjournals.org/content/20/6A/697.
14. R. Singh, J.W. Lillard, Nanoparticle-based targeted drug delivery, Exp. Mol. Pathol. 86 (2009) 215–223, https://doi.org/10.1016/j.yexmp.2008.12.004.
15. Lieber, C. M., & Chen, C. C. (1994). Preparation of Fullerenes and Fullerene-Based Materials. Solid State Physics - Advances in Research and Applications, 48(C), 109–148. https://doi.org/10.1016/S0081-1947(08)60578-0.
16. Luo, Y., Ren, C., Wang, S., Li, S., Zhang, P., Yu, J., Tang, W. (2018). Adsorption of Transition Metals on Black Phosphorene: a First-Principles Study. *Nanoscale Research Letters*, *13*. https://doi.org/10.1186/s11671-018-2696-x.

17. Sun, M., Tang, W., Ren, Q., Zhao, Y., Wang, S., Yu, J., Hao, Y. (2016). Electronic and magnetic behaviors of graphene with 5d series transition metal atom substitutions: A first-principles study. *Physica E: Low-Dimensional Systems and Nanostructures*, *80*, 142–148. https://doi.org/10.1016/j.physe.2016.01.026.
18. Wang, S., & Yu, J. (2018). Magnetic Behaviors of 3d Transition Metal-Doped Silicane: a First-Principle Study. *Journal of Superconductivity and Novel Magnetism*, *31*(9), 2789–2795. https://doi.org/10.1007/s10948-017-4532-4.
19. Sun, M., Tang, W., Ren, Q., Zhao, Y., Wang, S., Yu, J., Hao, Y. (2016). Electronic and magnetic behaviors of graphene with 5d series transition metal atom substitutions: A first-principles study. *Physica E: Low-Dimensional Systems and Nanostructures*, *80*, 142–148. https://doi.org/10.1016/j.physe.2016.01.026.
20. Wang, S., & Yu, J. (2018). Magnetic Behaviors of 3d Transition Metal-Doped Silicane: a First-Principle Study. *Journal of Superconductivity and Novel Magnetism*, *31*(9), 2789–2795. https://doi.org/10.1007/s10948-017-4532-4.
21. Bilge, M. (2017). Adsorption Mechanism and Structural Investigation of Doped C60 FullerenesWith Pentylamine. ANADOLU UNIVERSITY JOURNAL OF SCIENCE AND TECHNOLOGY A - Applied Sciences and Engineering, 1–1. https://doi.org/10.18038/aubtda.281646.
22. Soltani, A., Peyghan, A. A., & Bagheri, Z. (2013). H2O2 adsorption on the BN and SiC nanotubes: A DFT study. Physica E: Low-Dimensional Systems and Nanostructures, 48, 176–180. https://doi.org/10.1016/j.physe.2013.01.007.
23. Gowri Sankar, P. A., & Udhayakumar, K. (2013). Electronic properties of boron and silicon doped (10, 0) zigzag single-walled carbon nanotube upon gas molecular adsorption: A DFT comparative study. Journal of Nanomaterials, 2013(2). https://doi.org/10.1155/2013/293936.
24. Mahdavifar, Z., & Haghbayan, M. (2012). Theoretical investigation of pristine and functionalized AlN and SiC single walled nanotubes as an adsorption candidate for methane. Applied Surface Science, 263, 553–562. https://doi.org/10.1016/j.apsusc.2012.09.106.
25. Talla, J. A. (2012). Ab initio simulations of doped single-walled carbon nanotube sensors. Chemical Physics, 392(1), 71–77. https://doi.org/10.1016/j.chemphys.2011.10.014.
26. Gowri Sankar, P. A., & Udhayakumar, K. (2013). Electronic properties of boron and silicon doped (10, 0) zigzag single-walled carbon nanotube upon gas molecular adsorption: A DFT comparative study. Journal of Nanomaterials, 2013(December 2013), 0–13. https://doi.org/10.1155/2013/293936.
27. Reed, J. L. (1997). Electronegativity: Chemical hardness I. *Journal of Physical Chemistry A*, *101*(40), 7396–7400. https://doi.org/10.1021/jp9711050.
28. Pearson, R. G. (2006). Chemical hardness — A historical introduction. *Chemical Hardness*, *80*, 1–10. https://doi.org/10.1007/bfb0036796.
29. Ahmed Hassen Shntaif, Rashi, Z.M., Al-Sawaff, Z.H. *et al.* Quantum Chemical Calculations on Two Compounds of Proquazone and Proquazone Type Calcites as a Calcium Sensing Receptor (CaSR) Inhibitory Profiles. *Russ J Bioorg Chem* **47,** 777–783 (2021). https://doi.org/10.1134/S106816202103016X.
30. Zhao, Y., & Truhlar, D. G. (2008). The M06 suite of density functionals for main group thermochemistry , thermochemical kinetics , noncovalent interactions , excited states , and

transition elements : two new functionals and systematic testing of four M06-class functionals and 12 other functionals, 215–241.https://doi.org/10.1007/s00214-007-0310-x.
31. D.J.F. M. J. Frisch, G. W. Trucks, H. B. Schlegel, G. E. Scuseria, M. A. Robb, J. R. Cheeseman, G. Scalmani, V. Barone, B. Mennucci, G. A. Petersson, H. Nakatsuji, M. Caricato, X. Li, H. P. Hratchian, A. F. Izmaylov, J. Bloino, G. Zheng, J. L. Sonnenberg, M. Had, M.J. Frisch, G.W. Trucks, H.B. Schlegel, G.E. Scuseria, M.A. Robb, J.R. Cheeseman, G. Scalmani, V. Barone, B. Mennucci, G.A. Petersson, H. Nakatsuji, M. Caricato, X. Li, H.P. Hratchian, A.F. Izmaylov, J. Bloino, G. Zheng, J. L. Sonnenberg, M. Hada, M. Ehara, K. Toyota, R. Fukuda, J. Hasegawa, M. Ishida, T. Nakajima, Y. Honda, O. Kitao, H. Nakai, T. Vreven, J.A. Montgomery Jr., J.E. Peralta, F. Ogliaro, M. Bearpark, J.J. Heyd, E. Brothers, K.N. Kudin, V.N. Staroverov, R. Kobayashi, J. Normand, K. Raghavachari, A. Rendell, J.C. Burant, S. S. Iyengar, J. Tomasi, M. Cossi, N. Rega, J.M. Millam, M. Klene, J.E. Knox, J.B. Cross, V. Bakken, C. Adamo, J. Jaramillo, R. Gomperts, R.E. Stratmann, O. Yazyev, A.J. Austin, R. Cammi, C. Pomelli, J.W. Ochterski, R.L. Martin, K. Morokuma, V.G. Zakrzewski, G.A. Voth, P. Salvador, J.J. Dannenberg, S. Dapprich, A.D. Daniels, ¨O. Farkas, J.B. Foresman, J. V Ortiz, J. Cioslowski, D.J. Fox, Gaussian 09, Revision D.01, Gaussian Inc., Wallingford. (2013). DOI: https://10.1017/CBO9781107415324.004.
32. M.R. Hossain, M.M. Hasan, N.-E. Ashrafi, H. Rahman, M.S. Rahman, F. Ahmed, T. Ferdous, M.A. Hossain, Adsorption behaviour of metronidazole drug molecule on the surface of hydrogenated graphene, boron nitride and boron carbide nanosheets in gaseous and aqueous medium: A comparative DFT and QTAIM insight, Phys. E Low-Dimensional Syst. Nanostruct. 126 (2021), 114483, https://doi.org/10.1016/j.physe.2020.114483.
33. H. Rahman, M.R. Hossain, T. Ferdous, The recent advancement of low-dimensional nanostructured materials for drug delivery and drug sensing application: A brief review, J. Mol. Liq. 320-A (2020), 114427, https://doi.org/10.1016/j.molliq.2020.114427.
34. Bashiri, S., Vessally, E., Bekhradnia, A., Hosseinian, A., & Edjlali, L. (2017). Utility of extrinsic [60] fullerenes as work function type sensors for amphetamine drug detection: DFT studies. *Vacuum*, *136*, 156–162. https://doi.org/10.1016/j.vacuum.2016.12.003.
35. Al-sawaff, Z. ; Sayıner, H ; Kandemirli, F. . (2020). Quantum chemical study on two benzimidazole derivatives *1,2. Retrieved from https://dergipark.org.tr/en/pub/jauist/issue/55760/739466.
36. Kim, T. Il, Ri, C. Il, Yun, H. S., An, R. N., Han, G. B., Chae, S. Il, … Jon, Y. (2019). A Novel Method for Calculation of Molecular Energies and Charge Distributions by Thermodynamic Formalization. *Scientific Reports*, *9*(1), 1–12. https://doi.org/10.1038/s41598-019-56312-2.
37. Al-Sawaff, Z., Dalgic, S., & Kandemirli, F. (2021). Theoretical study of the adsorption of BMSF-BENZ drug for osteoporosis disease treatment on Al-doped carbon nanotubes (Al-CNT) as a drug delivery vehicle. *European Journal of Chemistry, 12*(3), 314-322. doi:10.5155/eurjchem.12.3.314-322.2143.
38. Gázquez, J. L. (2006). Hardness and softness in density functional theory. *Chemical Hardness*, *80*, 27–43. https://doi.org/10.1007/bfb0036798.
39. Transport, E. (2016). Density of States, Fermi Energy, and Energy Bands. *Thermoelectrics: Design and Materials*, 189–205. https://doi.org/10.1002/9781118848944.ch11.

40. M. Zou, J. Zhang, J. Chen, X. Li, Simulating adsorption of organic pollutants on finite (8,0) single-walled carbon nanotubes in water, Environ. Sci. Technol. 46 (2012) 8887–8894, https://doi.org/10.1021/es301370f.
41. J. Li, Y. Lu, Q. Ye, M. Cinke, J. Han, M. Meyyappan, Carbon Nanotube Sensors for Gas and Organic Vapor Detection, Nano Lett. 3 (2003) 929–933, https://doi.org/10.1021/nl034220x.
42. Lu, T., & Chen, F. (2012). Multiwfn: A multifunctional wavefunction analyzer. Journal of Computational Chemistry, 33(5), 580–592. https://doi.org/10.1002/jcc.22885.
43. Sözbilir, M., Pinarbaşi, T., & Canpolat, N. (2010). Prospective chemistry teachers' conceptions of chemical thermodynamics and kinetics. Eurasia Journal of Mathematics, Science and Technology Education, 6(2), 111–121.https://doi.org/10.12973/ejmste/75232.
44. Bagheri Novir, S., & Aram, M. R. (2021). Quantum mechanical studies of the adsorption of Remdesivir, as an effective drug for treatment of COVID-19, on the surface of pristine, COOH-functionalized and S-, Si- and Al- doped carbon nanotubes. *Physica E: Low-Dimensional Systems and Nanostructures*, *129*(February), 114668. https://doi.org/10.1016/j.physe.2021.114668.
45. S.U.D. Shamim, T. Hussain, M.R. Hossian, M.K. Hossain, F. Ahmed, T. Ferdous, M. A. Hossain, A DFT study on the geometrical structures, electronic, and spectroscopic properties of inverse sandwich monocyclic boron nanoclusters ConBm (n = 1.2; m = 6–8), J. Mol. Model. 26 (2020) 1–17, https://doi.org/10.1007/s00894-020-04419-z.
46. M. Rezaei-Sameti, S.K. Abdoli, The capability of the pristine and (Sc, Ti) doped Be12O12 nanocluster to detect and adsorb of Mercaptopyridine molecule: A first principle study, J. Mol. Struct. 1205 (2020), 127593, https://doi.org/10.1016/j.molstruc.2019.127593.
47. M. Shahabi, H. Raissi, Screening of the structural, topological, and electronic properties of the functionalized Graphene nanosheets as potential Tegafur anticancer drug carriers using DFT method, J. Biomol. Struct. Dyn. 36 (2018) 2517–2529, https://doi.org/10.1080/07391102.2017.1360209.